Journal of Organometallic Chemistry, 470 (1994) 275–283

A ^{197}Au Mössbauer study of reaction products of trimeric 1-benzyl-2-gold(I)-imidazole leading to Au^{I} carbene or Au^{I} imidazoline complexes and trinuclear Au^{III} imidazolyl derivatives. X-Ray crystal structure of $[\{(\mu\text{-1-benzylimidazolato-}N^3,C^2)Au\}_3I_2]$

Bruna Bovio

Dipartimento di Chimica Generale, Università, I-27100 Pavia (Italy)

Sandro Calogero

Dipartimento di Chimica Fisica, Università, I-30123 Venezia (Italy)

Friedrich E. Wagner

Physik-Department, Technische Universität München, D-85747 Garching (Germany)

Alfredo Burini and Bianca Rosa Pietroni

Dipartimento di Scienze Chimiche, Università, I-62032 Camerino (Italy)

(Received July 14, 1993)

Abstract

Reactions of the trinuclear $[Au_3Rim_3]$ compound (Rim = [μ-1-benzylimidazolato-N^3,C^2] with several reagents capable of oxidative addition have been investigated by ^{197}Au Mössbauer spectroscopy. The reaction products are either Au^{I} carbene mononuclear and binuclear complexes or trinuclear Au^{III} and mixed-valence compounds. The X-ray crystal structure of the mixed-valence complex $[Au^{III}Au^{I}_2Rim_3I_2]$ has been determined. Two two-coordinate Au^{I} centres show average Au–C and Au–N distances of 2.02(3) and 2.04(2) Å and average C–Au–N angles of 175.0(1.2)°, whereas the four-coordinate Au^{III} centre gives Au–C and Au–N 1.96(4) and 1.91(3) Å with the C–Au–N angle 170.5(1.6)°, and Au–I average distances 2.598(3) Å, with an I–Au–I angle 175.8(1)°. The Au–Au intramolecular distances [Au(1) ··· Au(2) 3.432(3), Au(1) ··· Au(3) 3.508(3), Au(2) ··· Au(3) 3.464(3) Å] indicate a weak metal–metal interaction.

Key words: Gold; Imidazole; Mössbauer spectroscopy; Crystal structure

1. Introduction

Oxidative addition to polynuclear gold(I) compounds has long been known [1]; it depends on several factors.

Firstly, on the structure: for example the oxidation reactions of dinuclear gold(I) ylide complexes with X_2 (I_2, Br_2, or Cl_2) or Ch_3I may give a transannular addition with formation of an Au^{II}–Au^{II} bond [2], whereas when three gold atoms are in a triangular array in a nine-membered ring, oxidation may occur at the three centres independently and the formation of metal–metal bonds is not observed [3].

Secondly, on the bridging ligands: for example trimeric derivatives of pyrazole [4] react with only one molecule of iodine to give a mixed-valence $Au^{III}/2Au^{I}$ compound [5–7], while the trimeric derivative $[\{AuC(OMe)=NMe\}_3]$ undergoes a stepwise addition with one, two or three molecules of halogen [3].

Correspondence to: Professor B. Bovio.

0022-328X/94/$7.00
SSDI 0022-328X(93)24181-3

Thirdly, on the reaction conditions: for example treatment of $[\{Au(\mu\text{-}3,5\text{-}Ph_2pz\}_3]$ with *aqua regia* affords a dinuclear gold(III) derivative $[[Cl_2Au\{\mu\text{-}(3,5\text{-}Ph_2\text{-}4\text{-}Cl\text{-}pyrazolato\text{-}N,N')\}]_2]$ [8a] or to a trinuclear mixed-valence $Au^{III}/2\ Au^{I}$ compound $[\{Au[\mu\text{-}(3,5\text{-}Ph_2\text{-}4\text{-}Cl\text{-}pz)\}_3Cl_2]$ [8b] depending on reaction time.

We therefore decided to investigate the behaviour of another type of trinuclear gold(I) compound, $[\{Au(\mu\text{-}Rim\text{-}N^3,C^2)\}_3]$, where Rim is 1-benzylimidazole, towards several reagents capable of oxidative addition.

In this work the reaction products **1–7**, prepared according to literature methods [9,10], were studied by ^{197}Au Mössbauer spectroscopy which provides a useful tool for elucidating the structure and bonding of gold compounds [11–13]; the results have been discussed on the basis of the available X-ray crystal data.

2. Results and discussion

All the samples except **4** were obtained by reaction of the cyclic trimeric compound **1** (see Scheme 1) with the appropriate reagent (ClCOOEt, PhCOCl, EtI, $SOCl_2$, or I_2). The final products **6** and **7** retain the cyclic nature of the starting material **1** and they are the

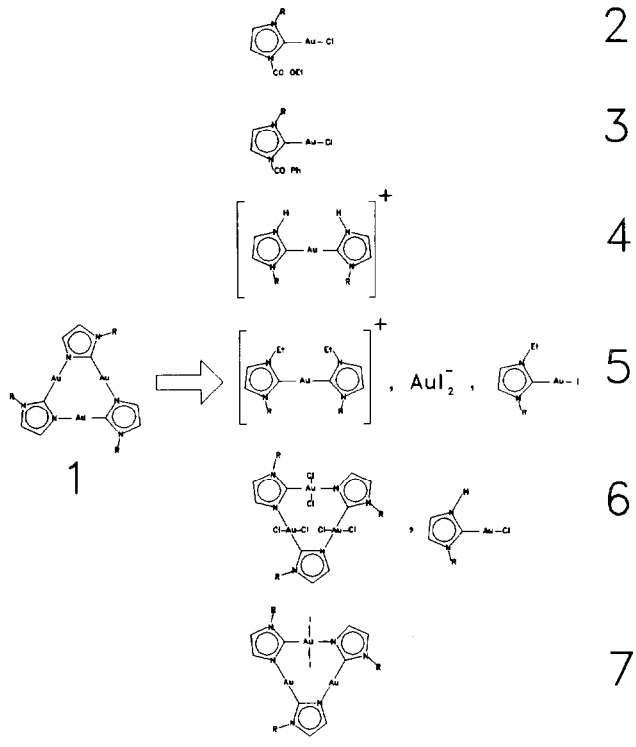

Scheme 1. Reaction scheme. Except for **4** [9], all the samples were prepared from the trinuclear starting material **1** (R = benzyl) [10].

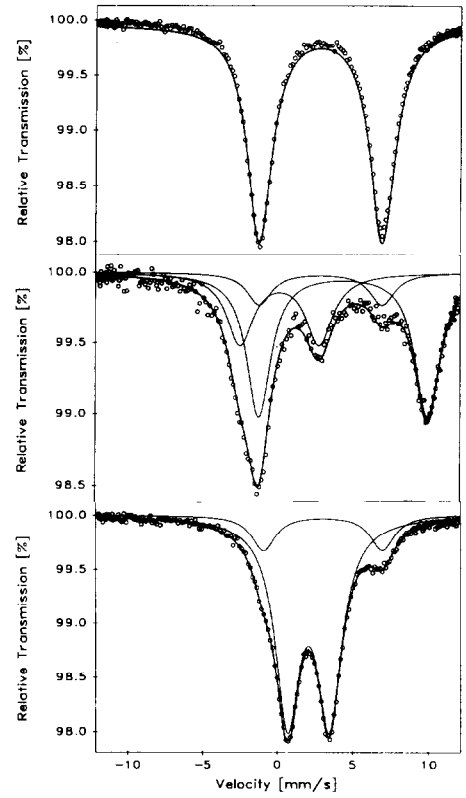

Fig. 1. Mössbauer spectra at 4.2 K for the samples **2**, **5** and **6**, from top to bottom. (Experimental points, small circles; envelope and sub-spectras, continuous lines).

result of oxidative addition to the metal [10]. In the other cases the reactions take another pathway and the trimeric complex **1** undergoes cleavage to give the carbene complexes **2**, **3**, **5** [10]. The carbene complex **4** was obtained by treating the intermediate of the reaction of lithium benzylimidazolate with Ph_3PAuCl in acidic media [9].

The samples **1–4** exhibit a typical Mössbauer spectrum consisting of one quadrupole-split doublet while the samples **5–7** exhibit two or three doublets (Fig. 1). The hyperfine Mössbauer parameters in mm s^{-1}, isomer shift IS and quadrupole splitting QS, are reported together with the average linewidth LW in Table 1. The linear correlations between QS and IS values [11] in Fig. 2 show that all the sites of the samples contain Au^{I}, except for the first site of samples **6** and **7** which contain Au^{III}.

The point-charge model has been used for clarifying the bonding mode of the ligands at Au^{I} coordination centres. The experimental electric quadrupole interactions have been calculated by employing the literature partial quadrupole spittings reported in the footnote of Table 2 [12,14]. Within the limits of the model, a substantial agreement between experimental and calcu-

TABLE 1. ^{197}Au Mössbauer parameters at 4.2 K

Sample [a]		IS [b]	QS	LW	
1	$[(Au^I)_3(im)_3$	3.87(1)	9.05(1)	2.02(1)	
2	$[Au^I im(COOEt)Cl)$	2.87(1)	8.09(1)	2.00(1)	
3	$[Au^I im(COPh)Cl)$	2.60(1)	7.58(2)	2.07(2)	
4	$[Au^I(imH)_2]^+$	4.40(1)	11.02(1)	2.02(1)	
5	$[Au^I(imEt)_2)^+$,	4.31(2)	11.12(4)	2.00(4)	58(1) [c]
	$[Au^I I_2)^-$,	0.20(3)	5.23(5)	2.29(7)	32(1) [c]
	$[Au^I(imEt)I]$	3.02(7)	7.80(9)	1.90(3)	10(1) [c]
6	$[(Au^{III})_3(im)_3Cl_6]$,	2.10(1)	2.79(1)	1.99(1)	86(1) [c]
	$[Au^I(imH)Cl)$	3.05(2)	7.86(4)	1.91(7)	14(1) [c]
7	$[Au^{III}Au^I_2(im)_3I_2]$	2.67(1)	3.70(2)	2.22(3)	48(1) [c]
		3.96(1)	9.26(2)	2.16(2)	52(1) [c]

[a] im = benzylimidazole; [b] relative to Au(Pt) source; [c] percentage of the gold site calculated by Mössbauer resonance area.

lated QS values is observed for the linear arrangements of Table 2.

With reference to Scheme 1, the starting trinuclear imidazolylgold(I) material **1** contains the linear arrangement C–Au–N as shown in Table 2.

The presence of the environment C–Au–Cl in samples **2** and **3** is evident from Table 2, consistent with the crystallographic data for mononuclear carbene complexes **2** [10] and **3** [15]. Table 1 implies a decrease in s-electron density at the gold nucleus and in p-electron asymmetry on going from **2** to **3**. The more negative shift is not due to COOEt or COPh since they have comparable donor powers and are far enough removed from the gold centre, but probably arises from the weak Au ··· Au interaction at 3.4308(4) Å in **3**. The increase in the Au–Cl bond length (from 2.271(3) in **2** to 2.286(2) Å in **3**) is due to this weak interaction; it means less electron charge donated to the gold and consequently a more negative shift. The C–Au–Cl bond angle variation from 179.9(3)° in **2** to 176.8(3)° in

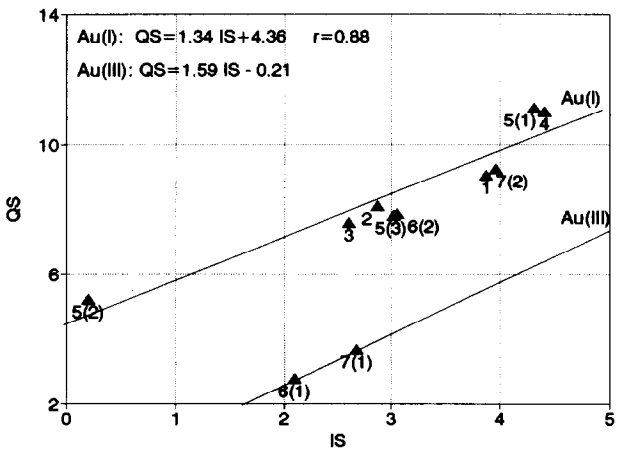

Fig. 2. Plot of QS *vs.* IS. The numbering of the samples is that of Table 1; the number in brackets indicates the gold site.

TABLE 2. Experimental and calculated quadrupole splittings for gold(I) sites

Sample [b]	QS	Calculated QS [a]				
		I–Au–I	C–Au–I	C–Au–Cl	C–Au–N	C–Au–C
1	9.05				−9.20	
2	8.09			−8.18		
3	7.58			−8.18		
4	11.02					−10.96
5	11.12					−10.96
	5.23	−5.36				
	7.80		−8.16			
6	7.86			−8.18		
7	9.26				−9.20	

[a] Partial quadrupole splittings, in mm s^{-1}: −1.35 for Cl and −1.34 for I [12]; −1.86 for N-ligand, *i.e.* the pyrazolate value calculated from the QS of Au_3(pyrazolato)$_3$, and −2.74 for C-ligands [14], *i.e.* the phenyl value calculated from the QS of Ph_3PAuPh; [b] The numbering of the samples is as in Table 1.

3 points to an increase in the gold coordination number, consistent with the observed decrease of the splitting. Within coordination number two, the C–Au–Cl variation from **2** to **3** is not enough to account for the splitting decrease. This is shown in Fig. 3 where the QS values, calculated by means of the point-charge formalism [16] are reported as a function of the angular variation. As a consequence the splitting decrease is not due to angular distortions but to an increased coordination number of the Au [17].

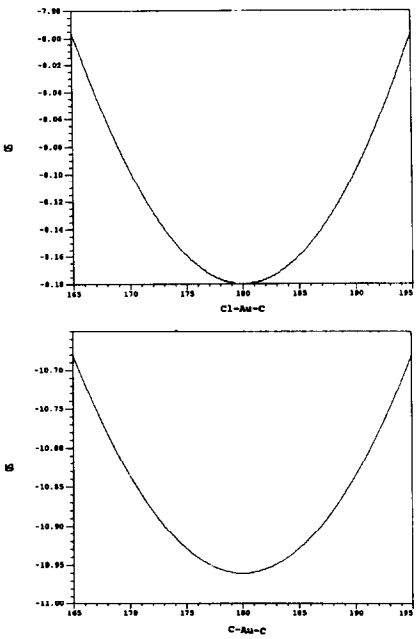

Fig. 3. QS values, calculated by point-charge model, *vs.* the values of the angles Cl–Au–C, for samples **2** and **3** (top), or C–Au–C for **4** (bottom).

Sample **4** and the first site of **5** exhibit the largest IS and QS values in Table 1. In these samples there is a large electron donation from the ligands to the gold which increases the population of the 6s and $6p_z$ gold orbitals. The 6s population produces a more positive IS and the $6p_z$ population increases the asymmetry in the p-orbitals. Table 2 demonstrates the presence of good σ-donor *C*-ligands in the gold environment of sample **4** and of the first site of **5**. The C–Au–C moiety belongs to the binuclear cation bis(1-benzylimidazolin-2-yliden)gold(I) whose crystal structure has been reported for the chloride derivative [9]. In this compound two Cl anions join two crystallographically non-equivalent cations: C–Au–C 175.2(4)° or 176.6(4)°, Au–C 2.01(1) and 2.02(1) Å, or 2.042(9) or 2.031(9) Å and with an interaction Au ··· Au at 3.2630(5) Å. The Mössbauer spectrum of sample **4** (Table 1) does not show two sites C–Au–C, but the point-charge model [16] shows that the angular values for the two C–Au–C sites are not different enough to produce an experimentally detectable splitting (Fig. 3).

Sample **5** also contains two other Au^I sites (Fig. 1). The second site of **5** (about 32%) may be assigned to $[AuI_2]^-$ whose Mössbauer parameters, IS 0.51 and QS 5.75 mm s^{-1} [18,19], are similar to those reported in Table 1. The third site of **5** (about 10%) is attributed in Table 2 to C–Au–I *i.e.* to the mononuclear derivative shown in Scheme 1.

The Mössbauer conclusions for sample **5** conflict with those obtained from ^1H and ^{13}C NMR and analytical data previously reported [10]. Therefore we recorded the ^1H NMR spectrum of sample **5** after γ irradiation. The presence of only one set of signals in the ^1H NMR spectrum rules out the possibility that there is more than one species in solution. The discrepancy between the results from the solid state and those from solution may be due to the solid state mixture being converted in solution in the carbene compound (1-benzyl-3-(ethyl)imidazolin-2-yliden]iodogold(I) [10].

The first site of the samples **6** or **7** has been attributed in Fig. 2 to square-planar gold(III) because of its hyperfine parameters. In addition the second site of **6** contains the moiety C–Au–Cl indicating that a carbene derivative with Mössbauer parameters close to those reported for **2** or **3** in Table 1 has been produced (about 14%) in a competitive reaction. As previously observed [12], the increase in the IS and QS values for the Au^{III} sites in **6** and **7** can be attributed to the increasing electron donation on going from Cl to I atoms. Any contribution due to the presence of Au^I or Au^{III} in the same molecule can be ruled out since the Mössbauer effect is a short range phenomenon.

The absence of the linear environment C–Au^I–N in sample **6** (Table 2) indicates that the three gold(I)

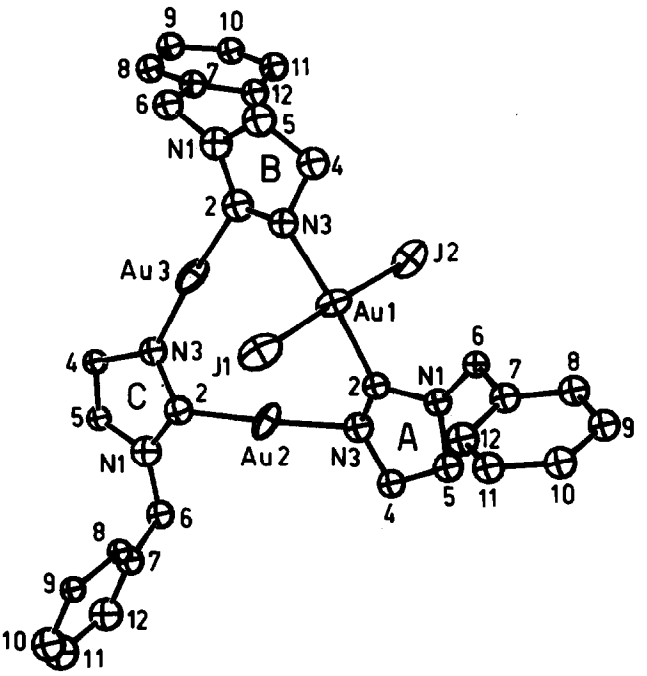

Fig. 4. ORTEP plot and numbering scheme of atoms. Thermal ellipsoids enclose 25% of the electron density. Hydrogen atoms are omitted for clarity.

centres of the starting material **1** have been oxidized to gold(III) (Scheme 1).

The Au^{III} and Au^I coordination sites in sample **7** are in the area ratio of about 1:1 assuming, as in Table 1, the same value for the recoil-free fraction f, but the Au^{III}/Au^I stoichiometric ratio is instead 1:2, as confirmed by the X-ray crystal structure. There is no real discrepancy between the Mössbauer and the X-ray results, because when Au^I and Au^{III} belong to the same molecular unit as in sample **7** the f-factor depends strongly on the intramolecular vibrational motions of the gold [20]. Consequently the f-factor ratio is closer to 2:1 and the Mössbauer area ratio is in close accord with the stoichiometric ratio of sample **7**. However, for sample **5** where Au^I is in three different molecular environments, or for sample **6**, where Au^{III} and Au^I are present in two different environments, the same f-factor has been assumed as a working approximation [20].

2.1. X-Ray crystal structure of [{(μ-1-benzylimidazolato-N^3,C^2)Au}$_3$$I_2$], 7

The structure of tris-μ-(1-benzylimidazolato-N^3,C^2)-diiodogold(III)digold(I), compound **7**, is represented in the ORTEP plot of Fig. 4 [21], together with the numbering scheme. It consists of discrete trinuclear molecules with the gold atoms bridged by three imidazolato-N^3,C^2 groups in a nine-membered ring. The two gold(I) atoms

are two-coordinate in a nearly linear arrangement and the gold(III) atom is four-coordinate with *trans* iodides in a nearly square planar arrangement. The least-squares plane passing through the atoms involved in the coordination of Au^{III} and the displacements of the atoms from it are: $-0.2687X' - 0.4384Y' - 0.8577Z' + 5.2042 = 0$ (X', Y', Z': orthogonal coordinates) Au(1) 0.021(2), I(1) −0.051(4), I(2) − 0.048(4), C(2A) 0.33(4), N(3B) 0.03(3) Å. The nine-membered ring is rather puckered. With respect to the least-squares plane passing through the atoms involved in the nine-membered ring: $0.0557X' + 0.9494Y' - 0.3091Z' - 1.5681 = 0$, the following out-of-plane displacements (Å) were observed: Au(1) 0.002(2), Au(2) 0.001(2), Au(3) −0.003(2), C(2A) −0.24(4), N(3A) −0.57(4), C(2B) −0.19(5), N(3B) 0.13(4), C(2C) 0.43(5), N(3C) 0.23(4) Å. Individual bond distances and angles are listed in Table 3 and their average values [22] in Table

TABLE 3. Interatomic distances (Å) and bond angles (deg) (with e.s.d.'s in parentheses)

Au(1)...Au(2)	3.432(3)	N(1)–C(6A)	1.46(5)
Au(1)...Au(3)	3.508(3)	C(6A)–C(7A)	1.54(6)
Au(2)...Au(3)	3.464(3)	N(1B)–C(2B)	1.39(6)
Au(1)–I(1)	2.595(4)	C(2B)–N(3B)	1.37(6)
Au(1)–I(2)	2.601(5)	N(3B)–C(4B)	1.40(6)
Au(1)–C(2A)	1.96(4)	C(4B)–C(5B)	1.40(7)
Au(1)–N(3B)	1.91(3)	C(5B)–N(1B)	1.41(6)
Au(2)–C(2C)	2.02(4)	N(1B)–C(6B)	1.48(6)
Au(2)–N(3A)	2.01(3)	C(6B)–C(7B)	1.57(7)
Au(3)–C(2B)	2.00(5)	N(1C)–C(2C)	1.39(6)
Au(3)–N(3C)	2.06(3)	C(2C)–N(3C)	1.40(6)
N(1A)–C(2A)	1.40(5)	N(3C)–C(4C)	1.40(5)
C(2A)–N(3A)	1.36(5)	C(4C)–C(5C)	1.40(5)
N(3A)–C(4A)	1.42(6)	C(5C)–N(1C)	1.39(5)
C(4A)–C(5A)	1.40(6)	N(1C)–C(6C)	1.43(6)
C(5A)–N(1A)	1.41(6)	C(6C)–C(7C)	1.50(7)
I(1)–Au(1)–I(2)	175.8(1)	N(1B)–C(2B)–N(3B)	108(4)
I(1)–Au(1)–C(2A)	91.6(1.3)	Au(3)–C(2B)–N(1B)	128.9(3.3)
I(1)–Au(1)–N(3B)	90.7(1.1)	Au(3)–C(2B)–N(3B)	116.9(3.3)
I(2)–Au(1)–C(2A)	86.1(1.3)	C(2B)–N(3B)–C(4B)	101(4)
I(2)–Au(1)–N(3B)	92.2(1.1)	Au(1)–N(3B)–C(2B)	126.2(3.0)
C(2A)–Au(1)–N(3B)	170.5(1.6)	Au(1)–N(3B)–C(4B)	121.2(2.7)
C(2C)–Au(2)–N(3A)	175.6(1.8)	C(3B)–C(4B)–C(5B)	103(4)
C(2B)–Au(3)–N(3C)	174.4(1.7)	C(4B)–C(5B)–N(1B)	103(4)
C(2A)–N(1A)–C(5A)	107(3)	N(1B)–C(6B)–C(7B)	112(4)
C(2A)–N(1A)–C(6A)	123(3)	C(6B)–C(7B)–C(8B)	117(4)
C(5A)–N(1A)–C(6A)	127(3)	C(6B)–C(7B)–C(12B)	124(4)
N(1A)–C(2A)–N(3A)	109(3)	C(2C)–N(1C)–C(5C)	107(3)
Au(1)–C(2A)–N(1A)	123.4(2.7)	C(2C)–N(1C)–C(6C)	127(4)
Au(1)–C(2A)–N(3A)	126.2(2.9)	C(5C)–N(1C)–C(6C)	126(4)
C(2A)–N(3A)–C(4A)	101(3)	N(1C)–C(2C)–N(3C)	109(4)
Au(2)–N(3A)–C(2A)	113.6(2.7)	Au(2)–C(2C)–N(1C)	128.0(3.2)
Au(2)–N(3A)–C(4A)	125.5(2.7)	Au(2)–C(2C)–N(3C)	119.9(2.9)
N(3A)–C(4A)–C(5A)	109(4)	C(2C)–N(3C)–C(4C)	104(3)
C(4A)–C(5A)–N(1A)	104(3)	Au(3)–N(3C)–C(2C)	119.4(2.6)
N(1A)–C(6A)–C(7A)	119(3)	Au(3)–N(3C)–C(4C)	133.9(2.7)
C(6A)–C(7A)–C(8A)	119(4)	N(3C)–C(4C)–C(5C)	107(3)
C(6A)–C(7A)–C(12A)	120(4)	C(4C)–C(5C)–N(1C)	106(3)
C(2B)–N(1B)–C(5B)	105(4)	N(1C)–C(6C)–C(7C)	116(4)
C(2B)–N(1B)–C(6B)	129(4)	C(6C)–C(7C)–C(8C)	122(4)
C(5B)–N(1B)–C(6B)	126(4)	C(6C)–C(7C)–C(12C)	120(4)
In the phenyl rings:			
Weighted averages of bond distances and endocyclic angles *:			
C(*joint*)–C(*ortho*)	1.41(3)	C(*ipso*)	119(2)
C(*ortho*)–C(*meta*)	1.42(3)	C(*ortho*)	120(2)
C(*meta*)–C(*para*)	1.41(3)	C(*meta*)	120(2)
		C(*para*)	120(3)

* The values were calculated according to A. Domenicano, A. Vaciago and C.A. Coulson, *Acta Crystallogr., B 31* (1975) 221.

TABLE 4. Average bond distances (Å) and angles (deg) with their standard errors [a]

	N	x_m	σ_m	σ'_m
Au^{III}–Au^{I}	2	3.467	0.038	0.002
Au^{III}–I	2	2.598	0.003	0.003
Au^{I}–N	2	2.036	0.020	0.024
Au^{I}–C	2	2.016	0.010	0.031
N(1)–C(2)	3	1.391	0.003	0.032
C(2)–N(3)	3	1.377	0.013	0.032
N(3)–C(4)	3	1.405	0.008	0.030
C(4)–C(5)	3	1.401	0.002	0.034
C(5)–N(1)	3	1.401	0.008	0.033
N(1)–C(6)	3	1.457	0.015	0.032
C(6)–C(7)	3	1.532	0.019	0.038
C–Au^{I}–N	2	175.0	0.6	1.2
Au^{I}–N–C(*end*)	2	116.6	2.9	1.9
Au^{I}–N–C(*eso*)	2	129.7	4.2	1.9
Au^{I}–C–N(*end*)	2	118.6	1.5	2.2
Au^{I}–C–N(*eso*)	2	128.4	0.5	2.3
C(2)–N(1)–C(5)	3	106.6	0.7	2.0
N(1)–C(2)–N(3)	3	108.5	0.3	2.1
C(2)–N(3)–C(4)	3	102.1	1.1	1.9
N(3)–C(4)–C(5)	3	106.6	1.8	2.0
C(4)–C(5)–N(1)	3	104.5	0.9	2.1
C(2)–N(1)–C(6)	3	126.0	1.6	2.0
C(5)–N(1)–C(6)	3	125.9	0.3	2.0
N(1)–C(6)–C(7)	3	115.9	2.1	2.1

[a] All values were calculated according to A. Domenicano, A. Vaciago and C.A. Coulson, *Acta Crystallogr., B31* (1975) 221.

4. The intramolecular Au ··· Au distances (3.432(3), 3.508(3) and 3.464(3) Å) indicate a weak metal–metal interaction, whereas the shortest intermolecular Au ··· Au approach (between Au(2) of X, Y, Z and Au(2) of −X, −Y, −Z) is 5.103(3) Å, thus excluding the formation of a pair of trimers of the sort of that found in [23].

The packing of the molecules in the crystal is determined by normal van der Waals contacts.

A comparison of structural features inside the nine-membered ring for this and for other related gold compounds is shown in Table 5.

The Au^{I}–N, 2.04(2) Å, and Au^{I}–C, 2.02(3) Å, average distances are nearly the same and longer than the corresponding ones in trinuclear gold-pyrazolate molecules. A possible reason for this difference may be the different *trans*-influences of imidazolato-N^3,C^2 and pyrazolato-N,N': the first has a significant *trans*-influence, higher than that of the chloride group [9,10]; the second has a weak *trans*-influence, comparable to that of the chloride group [24], because the imidazolate is a stronger σ-donor than the pyrazolate, consistent with the pKa values 7.1 for imidazole and 2.5 for pyrazole. Among the different pyrazolato-ligands, 3,5-bis(trifluoromethyl)pyrazolate might be expected to

TABLE 5. Comparison of structural parameters in trinuclear gold nine-membered metallocycles

	a [23]	b [24]	c [25]	d [26]	e [This work]
Distances (Å)					
Au^{I} ··· Au^{I}	3.27(2) *	3.348(3) *	3.368(1)	3.372(3)	3.464(3)
Au^{I} ··· Au^{III}				3.36(2) *	3.47(4) *
Au^{I}–N	2.03(1) *	1.93(1) *	1.978(9)	1.998(7) *	2.04(2) *
Au^{I}–C	1.96(1) *				2.02(3) *
Au^{III}–N				1.99(1) *	1.91(3)
Au^{III}–C					1.96(4)
N–C	1.31(5)				1.39(3) *
N–N		1.42(5) *	1.38(2)	1.39(2) *	
Angles (°)					
N–Au^{I}–C	175.0(1.0) *				175.0(1.2) *
N–Au^{I}–N		178.7(7) *	179.6(3)	178.5(5) *	
N–Au^{III}–C					170.5(1.6)
N–Au^{III}–N				179.6(8)	
Au^{I}–N–C	117.2(1.0)				116.6(2.9) *
Au^{I}–C–N	120.5(1.7)				118.6(2.2) *
Au^{I}–N–N		119.9(1.6) *	120.2(7)	118.8(7) *	
Au^{III}–N–C					126.2(3.0)
Au^{III}–C–N					126.2(2.9)
Au^{III}–N–N				120.6(1 .7) *	

a: [Au-μ-{1-(C_2H_5-O)-2-(CH_3-C_6H_4)CN}]$_3$
b: [Au-μ-{3,5-$(CF_3)_2C_3HN_2$}]$_3$
c: [Au-μ-{3,5-$(C_6H_5)_2C_3HN_2$}]$_3$
d: [Au-μ-{3,5-$(C_6H_5)_2C_3HN_2$}]$_3Cl_2$
e: [Au-μ-{1-(C_6H_5-CH_2)$C_3H_2N_2$}]$_3I_2$
* Weighted average values

have the weakest *trans*-influence, and indeed it produces an exceptionally short Au^I–N distance 1.93(1) Å [24].

The Au^{III}–N distance 1.91(3) Å is slightly shorter than the Au^{III}–C 1.96(4) Å and both are shorter than the corresponding distances with Au^I, unlike those in the $Au^{III}Au^I_2$ trimer d: average distances Au^{III}–N 1.99(1) and Au^I–N 1.998(7) Å [26]. The N–Au–C axes are bent outwards, especially N–Au^{III}–C (170.5(1.6)°), consistent with the large Au^{III}–N–C(endo) (126(3)°) and Au^{III}–C–N(endo) (126(3)°) angles.

The Au^{III}–I distances, 2.595(4) and 2.601(5) Å, are shorter than those in the mixed-valence $[\{AuCH_2P(S)(C_6H_5)_2I\}_2]$ [27]: 2.615(4) and 2.611(4) Å) and slightly shorter than those in $[Au^II_2]^-$ ions: 2.570(9) and 2.549(9) Å in $Rb_2[AgAu_3I_8]$ [28] or 2.564(3) Å in $K_2[Au_2I_6]$ [29].

As for the imidazole rings, the N–C (1.39(3)) and C–C (1.40(3) Å) average distances are slightly longer than in other metallated imidazoles [9,10,15,30,31], analogous to the observed but greater heterocycle "expansion" for tris[μ-3,5-bis(trifluoromethyl) pyrazolato-N,N']trigold(I) [24].

3. Experimental details

The samples **1**–**7** were prepared by the methods reported [9, 10]; their identities and purities were checked by elemental analyses, melting point determination, and ^{1}H NMR and infrared spectra.

The ^{1}H NMR spectra were always recorded again after the Mössbauer experiment, and no change was observed.

The crystal of the sample **7** used for the X-ray determination was obtained by slow diffusion of diethyl ether into a dichloromethane solution of the crude compound.

3.1. Mössbauer measurements

The ^{197}Pt activity feeding the 77.3 keV Mössbauer transition was produced by irradiation of isotopically enriched ^{196}Pt. Both source and absorber were kept at 4.2 K; a sinusoidal velocity waveform and an intrinsic Ge detector were used. The reported shifts are relative to the Au(Pt) source. An absorber thickness of 100 mg cm^{-2} was used. The fitting procedure was performed with the program MOS 90. The average linewidths of Table 1 are close to the minimum observable width of 1.87(3) mm s^{-1} for ^{197}Au [13], consistent with the presence of only one distinguishable gold site.

3.2. X-Ray analysis

The prismatic red crystal used for the X-ray diffraction measured approximately $0.07 \times 0.28 \times 0.49$ mm. Approximate unit-cell dimensions were derived by the SEARCH and INDEX programs from 25 measurements on a single crystal Enraf-Nonius CAD4 diffractometer with graphite monochromated Mo Kα radiation at the Centro Grandi Strumenti dell'Università, Pavia, Italy.

Accurate cell parameters were obtained by least-squares refinement of 2θ values of these reflections.

The triclinic cell quoted was confirmed by the use of the TRACER program [32] and a summary of crystal data is given in Table 6.

TABLE 6. Crystal data, data collection, and refinement of the structure

Formula	$C_{30}H_{27}N_6I_2Au_3$
Formula weight	1316.3
space group	$P\bar{1}$
colour	colourless
a, Å	12.989(5)
b, Å	14.248(9)
c, Å	10.408(5)
α, deg	94.28(5)
β, deg	101.95(4)
γ, deg	109.30(3)
V_c, Å^3	1757(2)
Z	2
D_{calcd}, g cm^{-3}	2.49
cryst. size, mm	$0.07\times0.49\times0.28$
μ (Mo Kα), cm^{-1}	147.1
data collcn. instrument	Enraf-Nonius CAD4
radiation (monochromated)	Mo Kα(λ = 0.7107 Å)
T of data collection, K	293
scan mode	$\omega/2\theta$
data collcn. range	$2 < \theta < 30$
no. of unique reflcns. measd.	9475 (h, $\pm k$, $\pm l$)
no. of data with $F_0^2 \geq 3\sigma(F_0^2)$	2712
no. of param refined	370
R [a] and R_w [b]	0.055, 0.064

[a] $R = (\Sigma||F_o| - k|F_c||)/\Sigma|F_o|$
[b] $R_w = \Sigma w(|F_o| - k|F_c|)^2/\Sigma w|F_o|^2]^{1/2}$.

The intensities of 9475 independent reflections were collected at room temperature with the $\omega/2\theta$ scan mode, within the angular range $2 < \theta < 30°$. The intensities of three standard reflections monitored every 300 min showed negligible variations. The intensities were corrected for Lorentz and polarization effects, and for absorption [33]. The structure factors were put on an absolute scale [34] and an overall isotropic thermal factor of 3.545 Å^2 was obtained thereby.

2712 reflections having $I \geq 3\sigma(I)$ were considered observed and used in the structure analysis.

3.3. Structure determination and refinement

The structure was solved by Patterson and Fourier methods and refined with anisotropic Au, N, C atoms and hydrogen atoms at calculated positions with the B_{iso} parameters of their bonded atoms down to R 0.055, R_w 0.064. At all stages of the structure analysis,

TABLE 7. Final coordinates (with esd's in parentheses)

Atom	x	y	z
Au(1)	0.2654(1)	0.2971(1)	0.3884(2)
Au(2)	0.0287(1)	0.1649(1)	0.1416(2)
Au(3)	0.2902(1)	0.2108(1)	0.0757(2)
I(1)	0.2311(3)	0.4465(2)	0.2816(4)
I(2)	0.2959(3)	0.1523(3)	0.5109(4)
N(1A)	0.0889(26)	0.2645(24)	0.5390(30)
C(2A)	0.1127(32)	0.2488(30)	0.4161(37)
N(3A)	0.0205(28)	0.1771(26)	0.3331(33)
C(4A)	−0.0675(33)	0.1950(31)	0.3807(38)
C(5A)	−0.0289(35)	0.2313(33)	0.5173(41)
C(6A)	0.1716(30)	0.3325(28)	0.6545(35)
C(7A)	0.1438(34)	0.4175(33)	0.7220(40)
C(8A)	0.1579(35)	0.4301(33)	0.8612(41)
C(9A)	0.1282(35)	0.5052(33)	0.9225(40)
C(10A)	0.0952(36)	0.5731(35)	0.8446(42)
C(11A)	0.0850(34)	0.5627(32)	0.7065(40)
C(12A)	0.1008(38)	0.4800(35)	0.6428(44)
N(1B)	0.5356(31)	0.3173(29)	0.2337(36)
C(2B)	0.4225(39)	0.2759(36)	0.2318(45)
N(3B)	0.4047(27)	0.3262(25)	0.3372(31)
C(4B)	0.5061(37)	0.3465(35)	0.4314(44)
C(5B)	0.5863(41)	0.3803(39)	0.3580(48)
C(6B)	0.5964(36)	0.2896(34)	0.1403(42)
C(7B)	0.6107(33)	0.1861(31)	0.1581(38)
C(8B)	0.6303(34)	0.1355(32)	0.0506(40)
C(9B)	0.6530(35)	0.0456(33)	0.0667(41)
C(10B)	0.6324(35)	−0.0057(33)	0.1766(41)
C(11B)	0.6096(36)	0.0427(33)	0.2817(42)
C(12B)	0.5816(34)	0.1308(32)	0.2620(39)
N(1C)	−0.0436(31)	0.0963(29)	−0.1613(36)
C(2C)	0.0419(35)	0.1444(33)	−0.0480(41)
N(3C)	0.1450(27)	0.1474(26)	−0.0731(32)
C(4C)	0.1223(29)	0.1283(28)	−0.2116(34)
C(5C)	0.0066(30)	0.0738(29)	−0.2590(35)
C(6C)	−0.1618(35)	0.0681(33)	−0.1742(40)
C(7C)	−0.2138(34)	0.1419(32)	−0.2245(39)
C(8C)	−0.1593(29)	0.2451(27)	−0.1887(33)
C(9C)	−0.1955(30)	0.3098(28)	−0.2679(34)
C(10C)	−0.3011(41)	0.2738(39)	−0.3634(48)
C(11C)	−0.3574(46)	0.1710(42)	−0.3990(53)
C(12C)	−0.3186(42)	0.1067(40)	−0.3194(50)

the observed reflections were given unit weight. Weights obtained from counting statistics did not lead to better results. The final difference Fourier map showed maximum and minimum $\Delta\rho$ values 1.93 and 1.43 eÅ^{-3}. The accuracy of this structure determination was limited by the poor quality of the crystals together with the not very accurate light atom positions in the presence of gold, as noted by Jones [35].

All calculations were carried out with the Enraf-Nonius SDP crystallographic computing package [36] and with local programs.

The final atomic positional parameters are listed in Table 7.

4. Supplementary material available

Tables of thermal parameters, positions of hydrogen atoms, interatomic distances and bond angles involving hydrogen atoms, are available from the Cambridge Crystallographic Data Centre, and these, plus a list of structure factors, can also be obtained from B.B.

Acknowledgments

Financial support from the "Consiglio Nazionale delle Ricerche" (Roma), MURST, and NATO (CRG 920179 to S.C. and F.E.W.) is gratefully acknowledged.

References

1 (a) R.J. Puddephatt, *The Chemistry of Gold*, Elsevier, Amsterdam, 1978, pp. 201–203, 109–119 and 137–138; (b) H. Schmidbaur and P. Jandik, *Inorg. Chim. Acta, 74* (1983) 97; (c) M.N.I. Khan, S. Wang and J.P. Fackler, Jr., *Inorg. Chem., 28* (1989) 3579; (d) C. King, D.D. Heinrich, G. Garzon, J.C. Wang and J.P. Fackler, Jr., *J. Am. Chem. Soc., 111* (1989) 2300; (e) R.G. Raptis, L.C. Porter, R.J. Emrich, H.H. Murray and J.P. Fackler, Jr., *Inorg. Chem., 29* (1990) 4408.
2 H. Schmidbaur and R. Franke, *Inorg. Chim. Acta, 13* (1975) 85.
3 A.L. Balch and D.J. Doonan, *J. Organomet. Chem., 131* (1977) 137.
4 F. Bonati, G. Minghetti and G. Banditelli, *J. Chem. Soc. Chem. Commun.*, (1974) 88.
5 G. Minghetti, G. Banditelli and F. Bonati, *Inorg. Chem., 18* (1979) 658.
6 M. Katada, K. Sako, Y. Uchida, S. Iijima, H. Sano, H.H. Wei, H. Sakai and Y. Maeda, *Bull. Chem. Soc. Jpn., 56* (1983) 945.
7 Y. Uchida, M. Katada, H. Sano, H. Sakai and Y. Maeda, *J. Radioanal. Nucl. Chem. Lett., 94* (1985) 215.
8 (a) A.L. Bandini, G. Banditelli, F. Bonati, G. Minghetti and M.T. Pinillos, *Inorg. Chim. Acta, 99* (1985) 165; (b) R.G. Raptis and J.P. Fackler, Jr., *Inorg. Chem., 29* (1990) 5003.
9 F. Bonati, A. Burini, B.R. Pietroni and B. Bovio, *J. Organomet. Chem., 375* (1989) 147.
10 F. Bonati, A. Burini, B.R. Pietroni and B. Bovio, *J. Organomet. Chem., 408* (1991) 271.
11 P. Guetlich, R. Link, A. Trautwein, in *Mössbauer Spectroscopy and Transition Metal Chemistry*, Springer-Verlag, Berlin, 1978, p. 201.
12 R.V. Parish, in G.J. Long (ed.), *Mössbauer Spectroscopy Applied to Inorganic Chemistry, Vol. 1*, Plenum Press, New York, 1984, p. 577.
13 H.D. Bartunik and G. Kaindl, in F.E. Wagner and Shenoy (eds.), *Mössbauer Isomer Shifts*, North-Holland Publishing Company, 1978, p. 517.
14 F. Bonati, A. Burini, B.R. Pietroni, S. Calogero and F.E. Wagner, *J. Organomet. Chem., 309* (1986) 363.
15 B. Bovio, A. Burini and B.R. Pietroni, *J. Organomet. Chem., 452* (1993) 287.
16 S. Calogero and C.D'Arrigo, Quantum Chemistry Program Exchange, Indiana University, Newsletter, (1978) 63.
17 G.C.H. Jones, P.G. Jones and A.G. Maddock, M.J. Mays, P.A. Vergnano, A.F. Williams, *J. Chem. Soc., Dalton Trans.*, (1977) 1440.
18 R.V. Parish, O. Parr and C.A. McAuliffe, *J. Chem. Soc., Dalton Trans.*, (1981) 2098.

19 A.K.H. Al-Sa'ady, C.A. McAuliffe, K. Moss, R.V Parish and R. Fields, *J. Chem. Soc., Dalton Trans.*, (1984) 491.
20 H. Schmidbaur, C. Hartmann and F.E. Wagner, *Angew. Chem., Int. Ed. Engl., 11* (1987) 26.
21 C.K. Johnson, ORTEP, Report ORNL-3793, Oak Ridge National Laboratory, TN, USA, 1965.
22 A. Domenicano, A. Vaciago and C.A. Coulson, *Acta Crystallogr., B31* (1975) 221.
23 A. Tiripicchio, M. Tiripicchio Camellini and G. Minghetti, *J. Organomet. Chem., 171* (1979) 399.
24 B. Bovio, F. Bonati and G. Banditelli, *Inorg. Chim. Acta, 87* (1984) 25.
25 H.H. Murray, R.G. Raptis and J.P. Fackler, Jr., *Inorg. Chem., 27* (1988) 26.
26 R.G. Raptis, H.H. Murray and J.P. Fackler, Jr., *Acta Crystallogr., C44* (1988) 970.
27 A.M. Mazany and J.P. Fackler, Jr., *J. Am. Chem. Soc., 106* (1984) 801.
28 W. Werner and J. Straehle, *Z. Naturforsch., 34b* (1979) 952.
29 J. Straele, J. Gelinek, M. Koelmel and A.M. Nemecek, *Z. Naturforsch., 34b* (1979) 1047.
30 B. Bovio et al, [(OC)$_2$Ir(μ-1-benzylimidazolyl-N^3, C^2]$_2$, crystal structure to be submitted for publication.
31 W.P. Fehlhammer, A. Voelkl, U. Plaia and G. Beck, *Chem. Ber., 120* (1987) 2031.
32 S.L. Lawton and R.A. Jacobson, TRACER, a cell reduction program, Ames Laboratory, Iowa State University of Science and Technology, Ames, IA, USA 1965.
33 A.C.T. North, D.C. Phillips and F.C. Mathews, *Acta Crystallogr., Sect. A, 24* (1968) 351.
34 A.J.C. Wilson, *Nature, Lond., 150* (1942) 152.
35 P.G. Jones, *Gold Bull., 14(3)* (1981) 112.